Hyperspectral Restoration based on Total Variation Regularized Low Rank Decomposition in Spectral Difference Space

Le Sun [a,b], Byeungwoo Jeon[a]
[a] School of Electronic and Electrical Engineering
Sungkyunkwan University
Suwon, South Korea
{sunlecncom, bjeon}@skku.edu

Yuhui Zheng[b]
[b] School of Computer and Software
Nanjing University of Information Science & Technology
Nanjing, P.R. China
zhengyh@vip.126.com

***Abstract*—This paper proposes a novel mixed noise removal method based on total variation regularized low rank decomposition in the spectral difference space (termed TVLRSDS) for hyperspectral imagery (HSI). Spectral difference transform has been demonstrated to be able to change the structure of noise (especially for the structured sparse noise, e.g., stripes or deadlines) in the original HSI, thus enabling low rank tools to effectively remove the mixed noise instead of treating it as one of the low rank components. In addition, as the fact that spectra in an HSI lie in a low dimensional subspace, and the adjacent pixels are highly correlative, it inspires us to simultaneously utilize the nuclear norm to exploit the global low rankness, and employ the total variation to include the local piecewise smoothness in the spectral difference space for mixed noise removal of HSI. The proposed model with all convex terms could be easily solved by alternating direction methods of multipliers (ADMM). The experimental results demonstrate the effectiveness of the proposed method.**

Keywords—hyperspectral denoising; total variation; low rank decomposition; spectral difference space; ADMM

I. INTRODUCTION

In past decades, the low rank technique has become a powerful tool in exploring the intrinsic structures of signals, especially for hyperspectral imagery (HSI). For instance, Lu *et al.* [1] proposed a low rank representation (LRR) method for HSI destriping. It utilized LRR for exploiting the high spectral correlation between different bands and then conducted a graph regularization for preserving the intrinsic local structure. Indeed, Zhang *et al.* [2] was the first to introduce LRR for HSI restoration based on low rank matrix recovery (LRMR) via so called "GoDec" algorithm [3] and made a big progress for HSI denoising. To overcome the drawback that LRMR only considers the local similarity within patches, the spectral nonlocal based LRR [4] and group LRR [5] were proposed to further improve the denoising performance. However, there are still two fatal flaws for those low rank based methods. One is 1) low rank methods are not good at removing heavy Gaussian noise due to its independent distribution, and the other is 2) low rank methods cannot remove the structured sparse noise, for example, when the deadlines or stripes are located at the same place in each band, low rank methods would treat them as one of the low-rank components and fail to remove them.

This work was supported by Natural Science Foundation of Jiangsu Province and China [BK20150923,61601236] and the NRF grants (NRF-2016R1D1A1B03934305. NRF-2017R1A2B2006518) and the Korean Research Fellowship Program (NRF-2015H1D3A1036067) both through the National Research Foundation of Korea (NRF) funded by the Ministry of Science and ICT.

978-1-5386-2615-3/18/$31.00 ©2018 IEEE

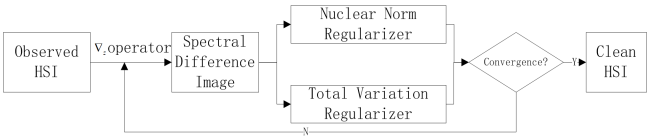

Fig.1. The flowchart of the proposed method

These two flaws significantly limit the performance of low rank methods. To overcome them, other techniques should be involved. Considering that total variation (TV) is a powerful and popular technique for suppressing Gaussian noise, band-by-band TV [6], structure tensor TV (STV) [7] and 3D TV [8] are combined with low rank techniques for mixed noise removal. Even these three methods improved the performance a lot for HSI mixed noise removal. However, the combination of LRR and band-by-band TV or STV still cannot remove the structured sparse noise completely, because TV regularization has one direction the same as the stripes or deadlines. 3DTV can help LRR technique to suppress the structured sparse noise by strengthening the weight in the spectral direction, however, it would result in spectra distortion. More recently, a method which enforces low rank representation on the spectral difference space (LRRSDS) [9] has drawn much attention in removing the structured mixed noise of HSI. However, one obvious drawback for LRRSDS is that it is not good at removing heavy Gaussian noise due to lack of spatial local correlation constraint.

By involving all advantages of these three kinds of techniques, in this paper, we propose to utilize total variation regularized low rank decomposition in spectral difference space, termed as TVLRSDS, to achieve a better result for HSI mixed noise removal, its flowchart is shown in Fig1.

II. BACKGROUND FORMULATION

The model for HSI mixed denoising based on low rank techniques could be formulated as [4]:

$$\min_{\mathbf{X},\mathbf{S}} \| \mathbf{Y}-\mathbf{X}-\mathbf{S} \|_F^2 + \lambda_1 \| \mathbf{S} \|_1 + \lambda_2 \| \mathbf{X} \|_* \qquad (1)$$

where $\mathbf{Y} \in \mathbb{R}^{(m\times n)\times l}$ is the observed HSI with $m\times n$ pixels and l bands, $\mathbf{X} \in \mathbb{R}^{(m\times n)\times l}$ is the desired clean HSI, $\mathbf{S} \in \mathbb{R}^{(m\times n)\times l}$ is the modeled sparse noise. $\|\mathbf{S}\|_1 = \sum |s_i|$ is the l_1 norm of the matrix $\mathbf{S}$

and s_i is its i th element. $\|\mathbf{X}\|_* = \sum|\sigma_i|$ is the nuclear norm which calculates the sum of singular values σ_i s of the matrix $\mathbf{X}$. Model (1) is the famous robust principal component analysis (RPCA) problem, it could be solved by several effective algorithms, e.g., inexact augmented Lagrange Multipliers [10] or "GoDec" [3].

To further improve the performance of LRMR, the low rank regularized total variation (LRTV) method was proposed by minimizing the following problem [6].

$$\begin{aligned} &\min_{\mathbf{X},\mathbf{S}} \|\mathbf{X}\|_* + \tau\|\mathbf{X}\|_{\mathrm{HTV}} + \lambda\|\mathbf{S}\|_1 \\ &s.t. \quad \|\mathbf{Y}-\mathbf{X}-\mathbf{S}\|_F^2 \le \varepsilon, \mathrm{rank}(\mathbf{X}) \le r \end{aligned} \tag{2}$$

where $\|\mathbf{X}\|_{\mathrm{HTV}} = \sum\|\hbar\mathbf{X}_j\|_{\mathrm{TV}} = \sum\{\|\nabla_h X\|_1 + \|\nabla_v X\|_1\}$ is the band-by-band TV, and $\mathbf{X}_j$ is the j th band of the HSI, $\hbar : \mathbb{R}^{mn} \to \mathbb{R}^{m\times n}$ denotes the operator that reshapes the vector of the j th band back to 2-D image, ∇_h and ∇_v denote the horizontal and vertical difference operators, respectively. Benefitting from the TV regularization, LRTV can produce more accurate results than LRMR, especially for Gaussian noise. However, for the structured sparse noise, both LRMR and LRTV cannot remove them completely.

III. Proposed Method

A. TVLRSDS Model

Spectral difference transform [9] supplies us a great opportunity to remove the structured sparse noise completely. Therefore, to remove Gaussian noise and structured sparse noise completely, we proposed to utilize TV regularized low rank decomposition in the spectral difference space for HSI mixed denoising. The proposed model is formulated as follows.

$$\begin{aligned} &\min_{\mathbf{X},\mathbf{S}} \|\mathbf{Y}-\mathbf{X}-\mathbf{S}\|_F^2 + \lambda_1\|\mathbf{S}\|_1 + \lambda_2(\|\nabla_z\mathbf{X}\|_{\mathrm{HTV},*}) \\ &\quad s.t. \quad \mathrm{rank}(\nabla_z\mathbf{X}) \le r \end{aligned} \tag{3}$$

where $\|\nabla_z\mathbf{X}\|_{\mathrm{HTV},*} \triangleq \|\nabla_z\mathbf{X}\|_* + \rho\|\nabla_z\mathbf{X}\|_{\mathrm{HTV}}$ is the proposed band-by-band TV regularized low rank decomposition term in the spectral difference space, which simultaneously enforces the local piecewise smoothness and the global low rankness, in the spectral difference space. The parameter ρ controls the contribution of this cross total variation term. $\|\nabla_z\mathbf{X}\|_{\mathrm{HTV}} = \|\nabla_h(\nabla_z\mathbf{X})\|_1 + \|\nabla_v(\nabla_z\mathbf{X})\|_1$, where ∇_z is the spectral difference operator. λ_1 and λ_2 are two parameters which balance the three terms.

The advantages of the model (3) are summarized as follows.

1) TV regularization could easily assist low rank technique to suppress the heavy Gaussian noise.

2) Spectral difference transform enables the TVLR term to further improve the performance in getting rid of the structured sparse noise.

3) All terms in the model (3) are convex, and it can be easily solved via ADMM method by splitting them into several simpler subproblems.

B. Optimization Algorithm

To effectively solve the optimization problem (3), we resort to ADMM method which minimizes the Lagrangian function of (3) by separating it into several simpler sub-problems. By letting $\mathbf{Q}_1=\nabla_z\mathbf{X}$, $\mathbf{Q}_2=\nabla_z\mathbf{X}$, $\mathbf{Q}_3=\nabla_h\mathbf{Q}_2$ and $\mathbf{Q}_4=\nabla_v\mathbf{Q}_2$, the Lagrangian function can be expressed as

$$\begin{aligned} \ell(\mathbf{X},\mathbf{S},\mathbf{Q}_1...,\mathbf{Q}_4) = &\min_{\mathbf{X},\mathbf{S},\mathbf{Q}_1...,\mathbf{Q}_4} \|\mathbf{Y}-\mathbf{X}-\mathbf{S}\|_F^2 + \lambda_1\|\mathbf{S}\|_1 \\ &+\lambda_2\{\|\mathbf{Q}_1\|_* + \rho(\|\mathbf{Q}_3\|_1 + \|\mathbf{Q}_4\|_1)\} \\ &+\mu\|\mathbf{Q}_1-\nabla_z\mathbf{X}-\mathbf{B}_1\|_F^2 + \mu\|\mathbf{Q}_2-\nabla_z\mathbf{X}-\mathbf{B}_2\|_F^2 \\ &+\mu\|\mathbf{Q}_3-\nabla_h\mathbf{Q}_2-\mathbf{B}_3\|_F^2 + \mu\|\mathbf{Q}_4-\nabla_v\mathbf{Q}_2-\mathbf{B}_4\|_F^2 \\ s.t. \quad &\mathrm{rank}(\mathbf{Q}_1) \le r \end{aligned} \tag{2}$$

where $\mathbf{B}_i, i=1,2,..,4$ are the Lagrangian multipliers and μ is the penalty parameter.

The pseudocode for solving the proposed TVLRSDS model by ADMM is summarized in Algorithm 1.

Algorithm 1: ADMM algorithm for TVLRSDS

Input: The observed HSI $\mathbf{Y}$, desired rank r, parameters λ_1 and λ_2, maximum iteration $k_{\max}$.

Output: The clean HSI $\mathbf{X}$.

1: **Initialization** $\mathbf{X}^{(0)}=\mathbf{S}^{(0)}=\mathbf{0}$, $\mathbf{Q}_i^{(0)}=\mathbf{0}$, $\mathbf{B}_i^{(0)}=\mathbf{0}$, μ=0.8, ρ=0.1 and $k=0$.

2:

3: **While** $k < k_{\max}$ or stopping criterion is not satisfied

4: $\mathbf{X}^{(k+1)} = \arg\min_{\mathbf{X}} \ell\left(\mathbf{X},\mathbf{S}^{(k)},\mathbf{Q}_i^{(k)},\mathbf{B}_i^{(k)}\right), i=1,2,3,4$

5: $\mathbf{S}^{(k+1)} = \mathrm{softTH}(\mathbf{Y}-\mathbf{X}^{(k+1)},\lambda_1)$

6: $\mathbf{Q}_i^{(k+1)} = \arg\min_{\mathbf{Q}_i} \ell\left(\mathbf{X}^{(k+1)},\mathbf{S}^{(k+1)},\mathbf{Q}_i,\mathbf{B}_i^{(k)}\right), i=1,2,3,4$

7: **Update multipliers**

8: $\mathbf{B}_1^{(k+1)} = \mathbf{B}_1^{(k)} + \nabla_z\mathbf{X}^{(k+1)} - \mathbf{Q}_1^{(k+1)}$

9: $\mathbf{B}_2^{(k+1)} = \mathbf{B}_2^{(k)} + \nabla_z\mathbf{X}^{(k+1)} - \mathbf{Q}_2^{(k+1)}$

9: $\mathbf{B}_3^{(k+1)} = \mathbf{B}_3^{(k)} + \nabla_h\mathbf{Q}_2^{(k+1)} - \mathbf{Q}_3^{(k+1)}$

9: $\mathbf{B}_4^{(k+1)} = \mathbf{B}_4^{(k)} + \nabla_v\mathbf{Q}_2^{(k+1)} - \mathbf{Q}_4^{(k+1)}$

10: **Update iteration** $k=k+1$

11: **End While**

Line 4 is related to the subproblem of $\mathbf{X}$, which is a convex problem and has a closed form solution by the fast Fourier transform (FFT). Line 5 is related to the subproblem of the sparse noise matrix $\mathbf{S}$, which can be easily solved by the soft threshold operator $\mathbf{S} = \mathrm{softTH}(\eta,\lambda_1) = \mathrm{sign}(\eta)\times\max\left\{0, |\eta| - \lambda_1/2\right\}$, where η=Y-X$^{(k+1)}$. Line 6 is related to the auxiliary variables $\mathbf{Q}_i$, and all these subproblems are convex and could be easily solved, more details for solving the corresponding subproblems can be found in [10,11].

The convergence of Algorithm 1 based on ADMM can be guaranteed theoretically in [12]. Moreover, the convergence rate of ADMM method depends on the parameters μ that is empirically set to 0.8 in the following experiments. It has been proven to converge effectively.

IV. Experimental Results

Both simulated and real HSI datasets were employed to evaluate the performance of the proposed method in the experiments. BM4D [13], LRMR [3], LRTV [6], 3DTVLR [8] and LRRSDS [9] were used to be its benchmark methods.

Moreover, the mean peak signal-to-noise ratio (MPSNR) index, the mean structural similarity (MSSIM) index, feature structural similarity (FSSIM), erreur relative globale adimensionnelle de sysnthese (ERGAS) [9], and the mean spectral angle (MSA) were determined for quantitative assessment of the results.

A. Experiments on Simulated Data Sets

The first experiment was conducted on the simulated Washington DC (WDC) mall data set. It has a 1-m spatial resolution and a 10-nm spectral resolution in the range of 0.4-2.5 μ m. A sub-image with the size of $256\times256\times191$ was used in the experiment. Before the simulation process, gray values of each band of WDC were mapped to [0,1]. To simulate the real case of noise-corrupted HSI, three kinds of noises were added to the dataset.

1) Zero-mean Gaussian noise with signal-to-noise ratio from 10-20 dB was added to each band randomly

2) Impulse noise with 20% density was randomly added to 20 bands

3) Dead lines were simulated for ten bands, in which five bands were chosen from the impulse noise bands and the other five bands were randomly chosen from the rest bands.

All parameters of the competing methods were set and tuned slightly according to the rules in the corresponding references. Moreover, all results are adopted based on the highest MPSNR index. For the proposed TVLRSDS, there are totally four parameters that are set to λ_1=0.01 , λ_2=0.1 , ρ=0.1 and $r=2$.

Fig 2 illustrates the denoising results of different methods in WDC data set. It is obvious that the proposed TVLRSDS removes all mixed noises and produces the best visual effect. For BM4D, it cannot remove the impulse noise and dead lines. LRMR can remove Gaussian noise and impulse noise, however, it fails to get rid of the structured dead lines completely. For LRTV, it performs as worse as BM4D does. Usually, when the dead lines or stripes have their own structure, LRTV fails to remove them. Even worse, there is always one band which seems to be not processed. For 3DTVLR, due to the unbalanced weights in each band, the dead lines in band 8 are not removed completely. For LRRSDS, due to lack of spatial constraint, Gaussian noise is not suppressed well.

Table I exhibits the results quantitatively. It gives the similar conclusion as that from Fig 2, that is, the proposed LRTVSDS produces the best results in all terms of MPSNR, MSSIM, FSSIM, ERGAS and MSA

As above analysis, there are totally 4 parameters in LRTVSDS method. In the course of experiment, we find that the parameters λ_1, λ_2 and r have the similar impact on the denoising results in WDC dataset as analyzed in [9]. Thus, we only plot the MPSNR and MSSIM as a function of the values of ρ, please see Fig 3. It leads us to conclude that when the values of ρ lie in the range of [0-0.1], LRTVSDS can produce the optimal results.

B. Experiments on Real Data Sets

The second experiment was conducted on the famous HYDICE dataset (namely Urban). The scene has the size of $256\times256\times210$, and is severely corrupted by Gaussian noise, stripes or dead lines.

Fig 4 illustrates the image of band 108 and the denoising

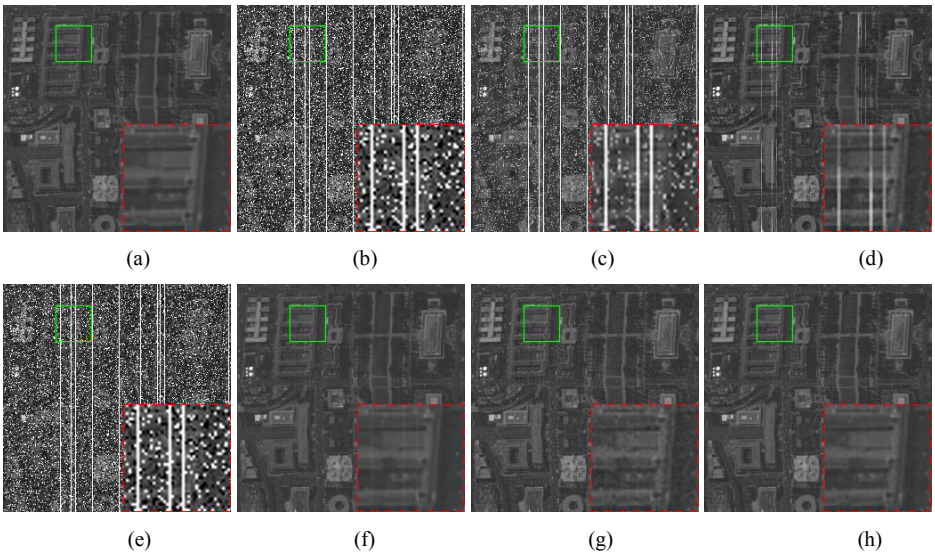

Fig. 2. Band 8 image of the denoising results in WDC dataset. (a) Clean image; (b) noisy image (PSNR =10.88 dB); (c) BM4D (PSNR =14.56 dB); (d) LRMR (PSNR =28.56 dB); (e) LRTV (PSNR = 12.16 dB); (f) 3DTVLR (PSNR =34.12 dB); (g) LRRSDS (PSNR =33.25 dB); (h) TVLRSDS (PSNR =35.89 dB).

TABLE I. ASSESSMENT METRICS FOR DIFFERENT DENOISING METHODS IN WDC DATASET

Metrics	Noisy	BM4D[13]	LRMR[3]	LRTV[6]	3DTVLR[8]	LRRSDS[9]	TVLRSDS
MPSNR(dB)	26.13	34.14	37.40	37.60	38.43	38.76	**39.29**
MSSIM	0.6957	0.8818	0.9699	0.9575	0.9723	0.9716	**0.9809**
FSSIM	0.8526	0.9388	0.9801	0.9727	0.9837	0.9852	**0.9887**
ERGAS	404.01	307.34	56.39	211.05	81.61	48.19	**45.58**
MSA	0.4434	0.2998	0.0693	0.1473	0.0896	0.0660	**0.0598**

results of competing methods. It is obviously seen that BM4D still performs poorly in removing strips. For the parts contaminated by heavy Gaussian noise, lots of fine details are oversmoothed. For LRMR and LRTV methods, they can remove Gaussian noise and impulse noise very well, however, both of them fail to get rid of the stripes. The main reason is that the stripes in Urban data set are located at the same place from band 100 to 109. The 3DTVLR can remove the stripes by strengthening the weight in spectral direction. In this way, the spectra produced by 3DTVLR are oversmoothed. For LRRSDS and TVLRSDS methods, they could remove all mixed noises and produce appealing results.

V. CONCLUSION

In this paper, we proposed a novel total variation regularized low rank decomposition method in the spectral difference space for HSI mixed noise removal. This proposed TVLRSDS method thoroughly exploits both spectral low rankness and spatial smoothness in the spectral difference space. It reveals the fact that TVLR term in the spectral difference space could significantly suppress heavy Gaussian noise and structured sparse noise. Extensive experimental results demonstrate that the proposed TVLRSDS solver outperforms several state-of-the-art denoising methods in removing mixed noises, especially for the structured sparse noise

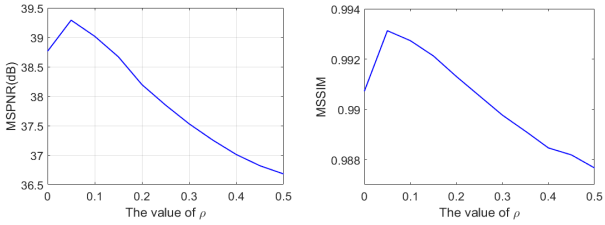

Fig.3. MPSNR and MSSIM as a function of the values of ρ .

REFERENCES

[1] X. Lu, Y. Wang, and Y. Yuan, "Graph-regularized low-rank representation for destriping of hyperspectral images," IEEE Trans. Geosci. Remote Sens., vol. 51, no. 7, pp. 4009−4018, Jul. 2013.

[2] H. Zhang, W. He, L. Zhang, H. Shen, and Q. Yuan, "Hyperspectral image restoration using low-rank matrix recovery," IEEE Trans. Geosci. Remote Sens., vol. 52, no. 8, pp. 4729−4743, Aug. 2014

[3] T. Zhou and D. Tao, "Godec: Randomized low-rank & sparse matrix decomposition in noisy case," in Proc. 28th ICML, 2011, pp. 33–40.

[4] R. Zhu, M. Dong, and J. Xue, "Spectral nonlocal restoration of hyperspectral images with low-rank property," IEEE J. Selected Top. Appl. Earth Observ. Remote Sen., vol. 8, no. 6, pp. 3062−3067, Jun. 2015.

[5] M. Wang, J. Yu, J. Xue, and W. Sun, "Denoising of hyperspectral images using group low-rank representation," IEEE J. Selected Top. Appl. Earth Observ. Remote Sen., vol. 9, no. 9, pp. 4420−4427, Mar. 2016

[6] W. He, H. Zhang, L. Zhang, and H. Shen, "Total-variation-regularized low-rank matrix factorization for hyperspectral image restoration," IEEE Trans. Geosci. Remote Sens., vol. 54, no. 1, pp. 178−188, Jan. 2016.

[7] Z. Wu, Q. Wang, J. Jin, and H. Shen, "Structure tensor total variation-regularized weighted nuclear norm minimization for hyperspectral image denoising. Signal Processing, vol. 131, pp. 202-219, 2017.

[8] L. Sun, Y. Zheng, and B. Jeon, "Hyperspectral restoration employing low rank and 3d total variation regularization. In Progress in Informatics and Computing (PIC), pp. 326-329, Dec. 2016.

[9] L. Sun, B. Jeon, Y. Zheng, and Z. Wu, "Hyperspectral image restoration using low-rank representation on spectral difference image," IEEE Geosci. Remote Sens. Lett., vol. 14, no. 7, pp. 1151-1155, July 2017.

[10] Z. Lin, M, Chen, and Y. Ma, "The augmented Lagrange multiplier method for exact recovery of corrupted low-rank matrices. Arxiv preprint arXiv: 1009.5055, 2010.

[11] L. Sun, B. Jeon, Y. Zheng, and Z. Wu, "A novel weighted cross total variation method for hyperspectral image mixed denoising", IEEE Access, vol. PP, no. 1, pp. 1-17, 2017

[12] J. Eckstein and W. Yao, "Understanding the convergence of the alternating direction method of multipliers: Theoretical and computational perspectives," Pacific J. Optim., vol. 11, no. 4, pp. 619–644, Jun. 2015.

[13] M. Maggioni, V. Katkovnik, K. Egiazarian, and A. Foi, "Nonlocal transform-domain filter for volumetric data denoising and reconstruction," IEEE Trans. Image Process., vol. 22, no. 1, pp. 119–133, Jan. 2013.

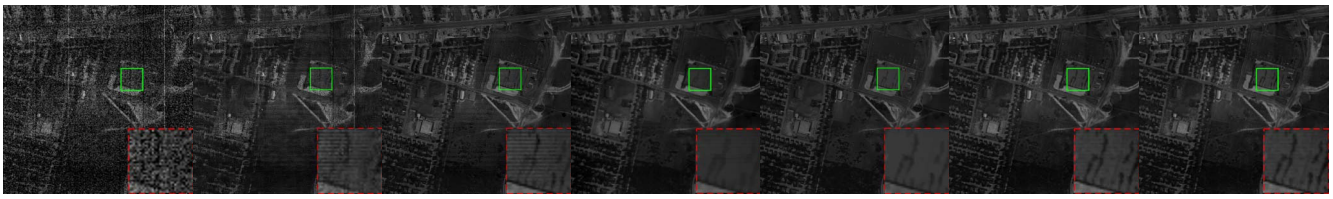

(a) (b) (c) (d) (e) (f) (g)

Fig. 4. Results of band 108 on Urban data set. (a) Clean image (b) BM4D (c) LRMR; (d) LRTV; (e) 3DTVLR; (f) LRRSDS; (g) TVLRSDS